

2004

Power Consideration in the Pulsed Dielectric Barrier Discharge at Atmospheric Pressure

M. Laroussi

Old Dominion University, mlarouss@odu.edu


X. Lu

V. Kolobov

R. Arslanbekov

Old Dominion University

Follow this and additional works at: https://digitalcommons.odu.edu/ece_fac_pubs

 Part of the [Electrical and Computer Engineering Commons](#), and the [Plasma and Beam Physics Commons](#)

Repository Citation

Laroussi, M.; Lu, X.; Kolobov, V.; and Arslanbekov, R., "Power Consideration in the Pulsed Dielectric Barrier Discharge at Atmospheric Pressure" (2004). *Electrical & Computer Engineering Faculty Publications*. 45.
https://digitalcommons.odu.edu/ece_fac_pubs/45

Original Publication Citation

Laroussi, M., Lu, X., Kolobov, V., & Arslanbekov, R. (2004). Power consideration in the pulsed dielectric barrier discharge at atmospheric pressure. *Journal of Applied Physics*, 96(5), 3028-3030.

Power consideration in the pulsed dielectric barrier discharge at atmospheric pressure

M. Laroussi, X. Lu, V. Kolobov, and R. Arslanbekov

Citation: [Journal of Applied Physics](#) **96**, 3028 (2004); doi: 10.1063/1.1777392

View online: <http://dx.doi.org/10.1063/1.1777392>

View Table of Contents: <http://scitation.aip.org/content/aip/journal/jap/96/5?ver=pdfcov>

Published by the [AIP Publishing](#)

Articles you may be interested in

[Investigation of ionized metal flux in enhanced high power impulse magnetron sputtering discharges](#)

J. Appl. Phys. **115**, 153301 (2014); 10.1063/1.4871635

[Characterization and mechanism studies of dielectric barrier discharges generated at atmospheric pressure](#)

Appl. Phys. Lett. **96**, 191503 (2010); 10.1063/1.3430008

[Self-pulsing 10⁴ A cm⁻² current density discharges in dielectric barrier Al / Al₂O₃ microplasma devices](#)

Appl. Phys. Lett. **94**, 011501 (2009); 10.1063/1.3064159

[Evidence of plasma-catalyst synergy in a low-pressure discharge](#)

Appl. Phys. Lett. **88**, 021503 (2006); 10.1063/1.2164915

[Optimization of ultraviolet emission and chemical species generation from a pulsed dielectric barrier discharge at atmospheric pressure](#)

J. Appl. Phys. **98**, 023301 (2005); 10.1063/1.1980530

The image shows the cover of an Applied Physics Reviews journal. It features a white background with a blue and orange border. The title 'AIP Applied Physics Reviews' is at the top. Below it is a diagram of a layered structure with labels 'A', 'B', and 'C'. The diagram shows a cross-section of a material with different layers and some internal structures. The background of the cover is a blue and orange gradient with some abstract shapes.

NEW Special Topic Sections

NOW ONLINE
Lithium Niobate Properties and Applications:
Reviews of Emerging Trends

AIP Applied Physics Reviews

Power consideration in the pulsed dielectric barrier discharge at atmospheric pressure

M. Laroussi^{a)} and X. Lu

Electrical and Computer Engineering Department, Center for Bioelectrics, Old Dominion University, Norfolk, Virginia 23529

V. Kolobov and R. Arslanbekov

CFD Research Corporation, Huntsville, Alabama 35805

(Received 5 March 2004; accepted 2 June 2004)

Nonequilibrium, atmospheric pressure discharges are rapidly becoming an important technological component in material processing applications. Amongst their attractive features is the ability to achieve enhanced gas phase chemistry without the need for elevated gas temperatures. To further enhance the plasma chemistry, pulsed operation with pulse widths in the nanoseconds range has been suggested. We report on a specially designed, dielectric barrier discharge based diffuse pulsed discharge and its electrical characteristics. Two current pulses corresponding to two consecutive discharges are generated per voltage pulse. The second discharge, which occurs at the falling edge of the voltage pulse, is induced by the charges stored on the electrode dielectric during the initial discharge. Therefore, the power supplied to ignite the first discharge is partly stored to later ignite a second discharge when the applied voltage decays. This process ultimately leads to a much improved power transfer to the plasma. © 2004 American Institute of Physics.
[DOI: 10.1063/1.1777392]

Dielectric barrier discharges (DBDs) are traditionally driven by sine wave voltages with magnitudes in the kV range and frequencies in the kHz range. Depending on the operating parameters, DBDs can generate either filamentary or diffuse plasmas. Both types of discharges have been found useful for a variety of applications, such as ozone generation,¹ vacuum ultraviolet radiation sources,² and biological sterilization.³ To improve the energy transfer efficiency, voltage pulses with sub-microsecond rise and fall times have been proposed by several investigators. Liu and Neiger⁴ have shown that at low pressures, two discharges are ignited per pulse: One at the rising edge and a second discharge at the falling edge of the voltage pulse. Here, we report experimental results showing that a similar mechanism occurs for a DBD operated at atmospheric pressure. Current measurements show two narrow current pulses, a positive one a short time after the voltage rising edge and a negative one at the falling edge of the voltage pulse. The negative current pulse is caused by the voltage induced by the charge accumulation on the dielectric during the first current pulse. These current pulses have peaks of few amperes and are about 100 ns wide. The total current (sum of the capacitive displacement current and the conduction current) and the discharge current are presented and discussed. The voltages across the dielectric and the gas gap are calculated and correlated to the current measurements. Finally, the different components of the power (stored and dissipated) are calculated and their impact on the power budget is elucidated.

A discharge device based on a modified DBD-type configuration is used in this study. It comprises two parallel electrodes separated by a gap. One of the electrodes is made of a 2 in. × 2 in. aluminum plate covered by an alumina (Al₂O₃) sheet. The dimensions of the Alumina sheet are: 75 × 75 × 1 mm³. The other electrode is made of a copper disk (diameter of 5.7 cm) with several holes through which the operating gas is injected. The diameter of the holes is about 1 mm. The distance between nearby holes is 5 mm. This electrode is not covered by a dielectric. The distance of the gap between the electrodes is adjustable from 1 mm to few centimeters. The gas flows out of the holes and into the discharge gap. Figure 1 is a schematic of the discharge setup. Figure 2 shows the experimental setup for the current-voltage measurements. The high voltage pulse generator is capable of producing pulses with amplitudes up to 10 kV, pulse widths variable from 200 ns to dc, and with a repetition rate up to 10 khz. The rise and fall times of the voltage pulses are about 100 ns. Voltages are measured by a P6015 Tektronix high voltage probe and currents by a A6312 Tektronix current probe. The voltage and current wave forms are viewed by a Tektronix TDS 784D wideband digital oscilloscope. For high pulse repetition rates and for adequately high voltages (the value of which depends on the gap distance) we were able to generate stable diffuse plasmas for both helium/air and argon/air gas mixtures.

Figure 3 shows the applied voltage pulse and the corresponding total current for a gap distance of 2.5 mm. Helium with about 1% mixture of air was used. The voltage pulse repetition rate is 1 khz. Two distinct current pulses are clearly visible. The first pulse occurs at the rising front of the voltage pulse and the second current pulse occurs at the falling front of the voltage. These current pulses include both

^{a)}Author to whom correspondence should be addressed; electronic mail: mlarouss@odu.edu

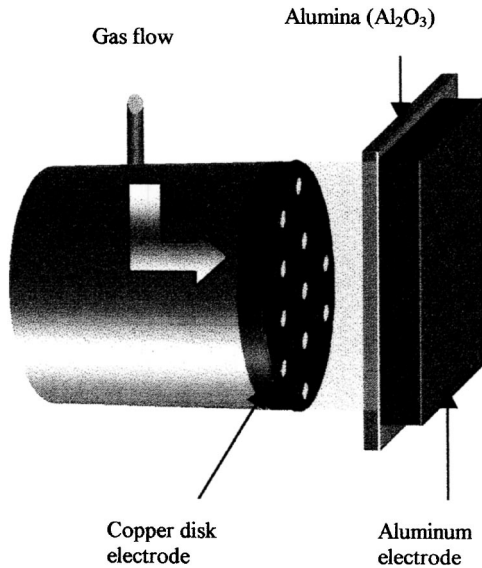


FIG. 1. Three-dimensional illustration of the DBD-based device used in the experiments.

the displacement current (which is also present when no plasma is generated) and the conduction current, which flows as soon as a conduction channel is formed when the gap breaks down (discharge ignition). To find the actual discharge current, the displacement current (due to cable capacitance, the dielectric capacitance, and the gas gap capacitance) is subtracted from the total measured current. The discharge electrical model used in our calculations is shown in Fig. 4. The capacitors C_{cable} (48 pF), C_d (145 pF), and C_g (calculated, 9 pF) represent the cable capacitance, the equivalent capacitance of the dielectric, and the equivalent capacitance of the gas gap. The displacement current is due to the combination of these capacitors. The resistance R_p represents the finite conductivity of the plasma and corresponds to power dissipation.

The discharge current is shown in Fig. 5. The first pulse of the discharge current starts after the applied voltage reaches a certain value, which depends on the gap distance. The delay between the start of the voltage pulse and that of the first discharge current pulse is about 100 ns. After the first pulse occurrence, the discharge current remains zero until the arrival of the falling front of the voltage. About 50 ns

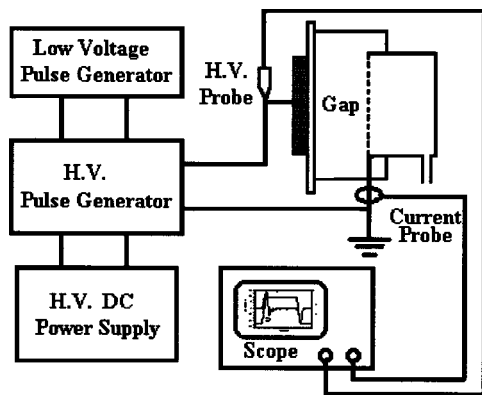


FIG. 2. Experimental setup of the discharge system with diagnostics.

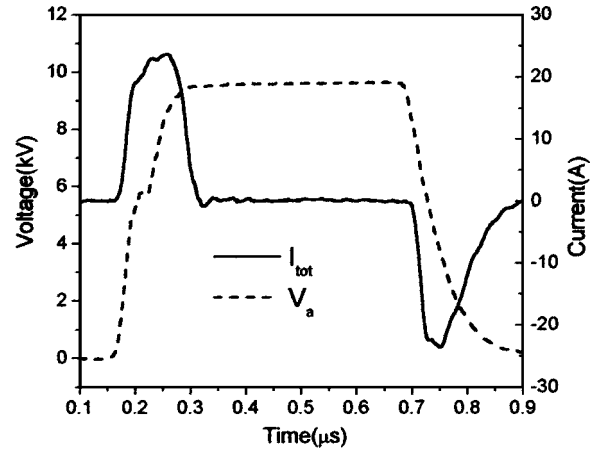


FIG. 3. Total current I_{tot} and applied voltage V_a vs time.

after the beginning of the falling front, a current pulse is observed. This corresponds to a second breakdown of the gap. This second discharge ignites because of the voltage induced by the charges, which have accumulated on the surface of the dielectric plate during the first discharge.

Figure 6 shows the applied voltage V_a , the voltage across the dielectric V_d , and the voltage across the discharge gap V_g (the locations of these voltages are shown in Fig. 4). The voltage across the dielectric is calculated by the ratio of the time integral of the current through the DBD, I_{DBD} , and the dielectric capacitance C_d ($C_d=145$ pF). The voltage across the gas gap is simply given by $V_g=V_a-V_d$. Note that V_g exhibits a negative pulse when the applied voltage V_a decays. This negative pulse is induced by the charges previously collected on the surface of the dielectric plate. The voltage across the dielectric, V_d , starts increasing only after the discharge is initiated (point 1 in Fig. 6), which is few nanoseconds after the rising front of the applied voltage pulse. Then V_d rises rapidly when the discharge current increases (point 2). This rise is due to charges from the plasma volume being collected on the surface of the dielectric. When the first discharge extinguishes, V_g goes to zero and V_d becomes equal to V_a and remains at that level until the arrival of the falling front of V_a , at which time (marked 3 in Fig. 6) V_g increases (negatively) and V_d starts decaying. The increase of the magnitude of V_g leads to the breakdown of the gap and initiation of a second discharge. At the point marked 4, the dielectric capacitance discharges itself rapidly through the plasma, the discharge extinguishes, and both V_d and V_g go to a zero value. When another pulse of the applied voltage arrives, the whole scenario described above is repeated again. Therefore increasing the repetition rate of the applied voltage leads to a

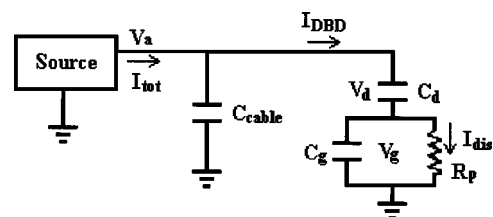


FIG. 4. Discharge model used for discharge current, dielectric voltage, and gas voltage calculations.

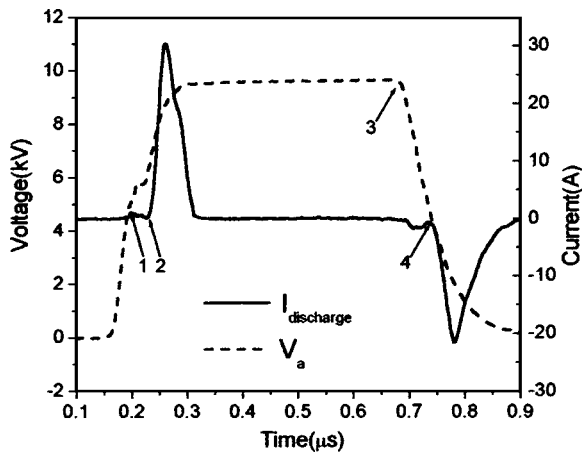


FIG. 5. Discharge current $I_{\text{discharge}}$ and applied voltage vs time. Points 1, 2, 3, and 4 correspond to the same marked points as in Fig. 6. These points correspond to characteristic times of discharge ignition (point 1 and point 4), beginning of the negative gas voltage pulse (point 3), and point of sharp increase in dielectric voltage and positive discharge current pulse (point 2).

higher frequency of occurrence of the double discharges and to a more temporally stable plasma.

Figure 7 shows the total power supplied or received by the power supply P_{supp} and the power dissipated in the plasma, P_{gas} . P_{supp} is the product of I_{tot} (shown in Fig. 3) and the applied voltage V_a . P_{gas} is the product of $I_{\text{discharge}}$ (shown in Fig. 5) and V_g (shown in Fig. 6). During the first rising front of the applied voltage P_{supp} includes both the power dissipated in the plasma and the reactive power stored in the various capacitors (cable, dielectric, and gas). At the falling front of the applied voltage the sign of P_{supp} is negative

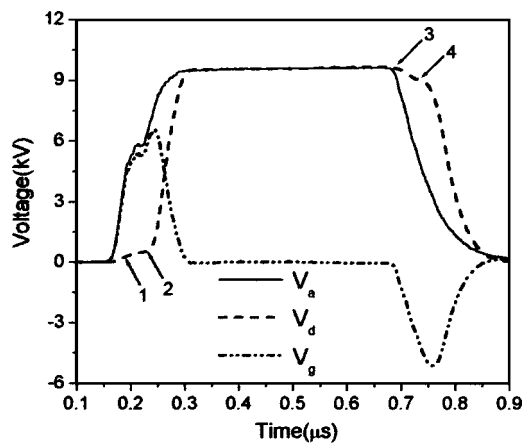


FIG. 6. Applied voltage V_a , dielectric voltage V_d , and gas voltage V_g vs time.

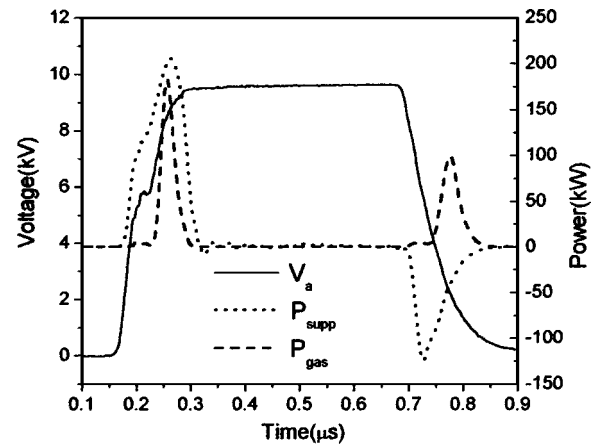


FIG. 7. Applied voltage, supply power P_{supp} , and gas dissipated power P_g vs time. When P_{supp} is positive the power is supplied from source to load, and when P_{supp} is negative the power is restored from load to source.

which represents a power returned to the power source. This “recuperated” power helps lower the power budget in the sense that some of the originally supplied power is restored to the source. The curve representing P_{gas} shows the power dissipated in the plasma during the first and the second discharges. What is of importance in this curve is the fact that the second discharge occurs without any power contribution from the power source.

In summary, we have shown that a relatively large volume diffuse DBD can be generated at atmospheric pressure with repetitive narrow voltage pulses. Two discharges are generated per single voltage pulse. The second discharge occurs without any power contribution from the driving source. This is because the power used to generate the first discharge is partly stored to generate a second one when the applied voltage decays. Although the power dissipated is in the kilowatt range, the actual energy needed is only few milli-Joules since the pulses are narrow (few hundred nanoseconds) and the power is transferred from source to load and vice versa only during the rise and fall times of the voltage pulse, which are few tens of nanoseconds long.

ACKNOWLEDGMENT

This work was partly supported by an AFOSR STTR grant.

¹B. Eliasson, M. Hirth, and U. Kogelschatz, *J. Phys. D* **20**, 1421 (1987).

²U. Kogelschatz, *Pure Appl. Chem.* **62**, 1667 (1990).

³M. Laroussi, *IEEE Trans. Plasma Sci.* **30**, 1409 (2002).

⁴S. Liu and M. Neiger, *J. Phys. D* **34**, 1632 (2001).